Available online at http://www.journalcra.com

International Journal of Current Research
Vol. 6, Issue, 06, pp.7032-7037, June, 2014

INTERNATIONAL JOURNAL OF CURRENT RESEARCH

ISSN: 0975-833X

RESEARCH ARTICLE

CRACK PROPAGATION AND FRACTURE ANALYSIS IN ENGINEERING STRUCTURE BY GENERATIVE PART STRUCTURAL ANALYSIS

[1*]Sushovan Chatterjee and [2]Bidyot Doley

[1]Department of Mechanical Engineering, National Institute of Technology Silchar, Assam-788010, India
[2]Assistant Manager-Engineering, Tata Toyo Radiator Ltd., Tata Auto Comp System Ltd Pune, India

ARTICLE INFO

Article History:
Received 18th March, 2014
Received in revised form
06th April, 2014
Accepted 09th May, 2014
Published online 25th June, 2014

Key words:
Critical crack length,
Stress intensity factor,
Stress concentration factor,
Crack propagation.

ABSTRACT

Crack propagation study is a viable and futuristic criterion to design better and more adaptive engineering structures; hence it becomes imperative to indulge in a concrete study of crack propagation. In this paper, CATIA V5 software is used as a tool for modeling and stress analysis, in order to estimate Critical crack length and the critical load. Further comparative study is done based on critical length between various engineering structures which are rectangular beam, I-beam, hollow shaft and solid shaft from which hollow shaft is been found better over the other structures for engineering design.

INTRODUCTION

Cracks are defects in engineering structure arising mainly due to flaw during manufacturing, and also due to their structural morphology. The crack initiation in different structures had been studied and the critical load and critical crack length were found out to check whether crack starts to propagate by computing the stress intensity factor (K_i). Cracks were assumed to propagate *via* a process of quasi-static incremental steps through the crack tip damage zone (Wang Zhiqiang and Nakamura Toshio 2004)), and the internal stresses decrease as a short crack grows out of the stress field (Sadananda and Vasudevan 1997). We have followed Irwin's Criterion of crack propagation. According to Irwin a crack can only propagate when the stress concentration factor (K) is equal to K_c which is the critical stress concentration factor at fracture (Gürses Ercan and Miehe Christian 2009). The growth of a crack requires the creation of two new surfaces and hence an increase in the surface energy (Curtin *et al.,* 2010). The fresh surface area produced in each fatigue cycle is in proportion to the crack propagation rate (Shimojo *et al.,* 1993). In ductile materials a plastic zone develops at the tip of the crack. As the applied load increases, the plastic zone increases in size until the crack grows and the material behind the crack tip unloads. The plastic loading and unloading cycle near the crack tip leads to the dissipation of energy as heat. Hence, a dissipative term has to be added to the energy balance relation (Miserez *et al.,* 2004). Crack propagation behavior is highly dependent on the variations of the failure parameters. In non-homogeneous materials, crack propagation in elastic–plastic graded materials never attains a steady state and the fracture energy associated with crack growth continues to vary as the crack propagates through the graded region (Hurley and Evans 2007). The crack propagation direction associated with the classical Griffith criterion is identified by the material configurational force which maximizes the local dissipation at the crack front (Seweryn Andrzej 1994).

Considered Model and Material Parameters

During this analysis, four engineering model structures were taken into consideration viz. Rectangular beam, I-section beam, Solid circular shaft, and Hollow circular shaft. Steel is being considered as the material for construction of the aforementioned structures having the mechanical properties as shown in Table 1.

Table1 . Material properties (as per catia v5 library)

Material	Steel
Young's modulus(N/m^2)	2×10^{11}
Poison's Ratio	0.266
Density(kg/m^3)	7860
Co-efficient of thermal expansion(/°C)	1.17×10^{-05}
Yield Strength (N/m^2)	2.5×10^{08}

Corresponding author: Sushovan Chatterjee
Department of Mechanical Engineering, National Institute of Technology Silchar, Assam-788010, India.

Analysis Procedure

Rectangular beam

In this case the objective has been framed to study and analyze the crack propagation in a rectangular beam for which a model element is created in CATIA V5. The dimensions of the beam are shown in the Fig.1.

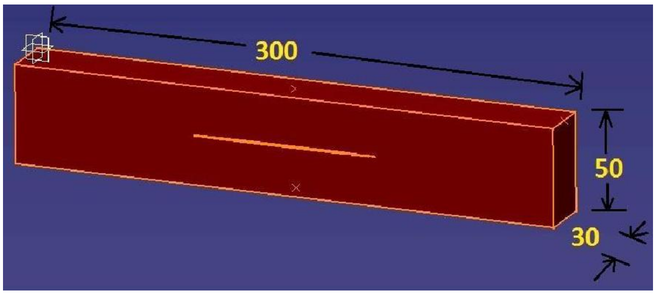

Fig. 1. Basic dimensions of the rectangular beam model element

Now the model is analysed with 18.736 *mm* mesh size 3.002 *mm* absolute sag, 42500 *N* point load. The blue part shows the less stress concentration, green part shows higher stress concentration and red part shows the highest stress concentration which is located on the crack as shown in Fig.2 and also in every model analysed in CATIA V5. Data were collected at different lengths.

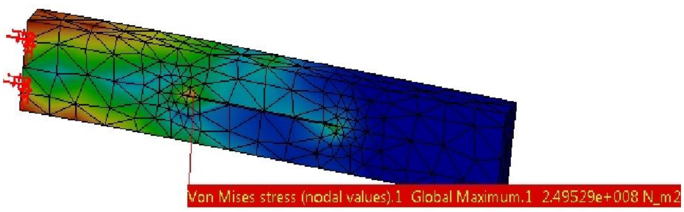

Fig. 2. Von Mises Stress Distribution of rectangular beam

The analysis from CATIA V5 has been shown in Table 2 for the rectangular beam. The red marked row of every table indicates the critical stress concentration factor and critical crack length.

Table 2. Result Analysis on Rectangular Beam

Sl. No.	Crack length (*mm*)	Stress (σ) N/m^2 x 10^{08}	*(K)* $Pa\ m^{1/2}$ x 10^{08}
1	80	1.83	0.65
2	90	2.26	0.85
3	98	2.50	0.99
4	100	2.72	1.08
5	110	2.69	1.12

The variation of stress concentration factor against the computational crack length reveals that there are sudden rise in stress concentration factor, when the crack length reaches at its critical value at 98 *mm* crack length as is evident from Fig.3.

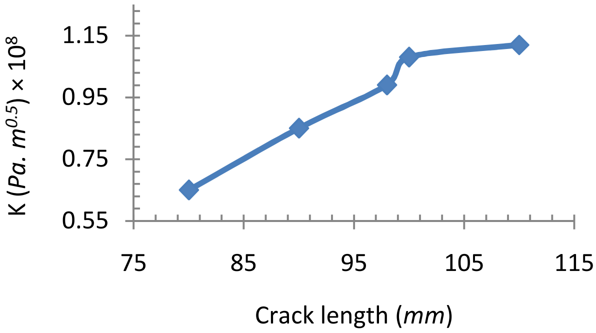

Fig. 3. Computational Crack length vs. Stress Concentration factor for rectangular beam

I-beam

The I-beam model has been considered having elliptical crack along the axis of the beam with the major axis of the crack and minor axis perpendicular to it. As shown in Fig.4.

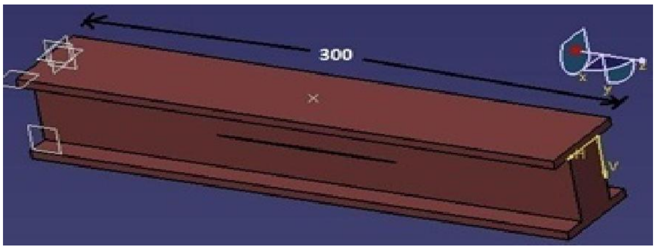

Fig. 4. Basic dimensions of the I-Beam model element.

Using the graphical interface of CATIA V5 the distribution of Von Mises stress has been plotted as shown in Fig.5.

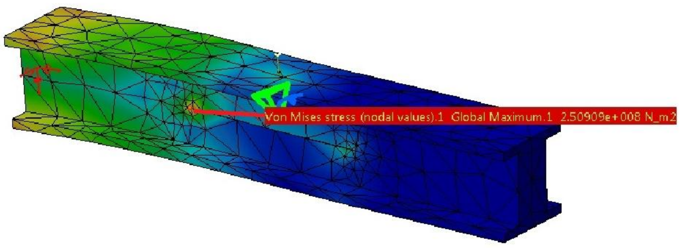

Fig. 5. Von Mises Stress Distribution of I-Beam

Here the mesh size is 18.736 *mm*, absolute sag 3.002 *mm* and point load 42500 *N*. The result of the analysis is given in Fig.5 and Table 3.

Table 3. Result Analysis on I-Beam Point Load

Sl. No.	Crack length (*mm*)	Stress (σ) N/m^2 x 10^{08}	*(K)* $Pa\ m^{1/2}$ x 10^{08}
1	80	1.13	0.40
2	90	2.15	0.81
3	100	2.50	0.99
4	110	2.62	1.09
5	120	2.53	1.10

The variation of *K* with Crack length is shown in Fig. 6.

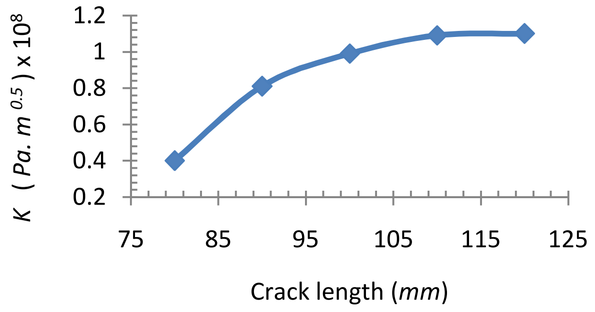

Fig. 6. Computational crack length vs. Stress Concentration Factor for I-beam

Now the I-Beam is subjected to rotational and point load both having crack type elliptical along the major axis diameter 25 *mm* and minor axis diameter 1 *mm* and at a distance of 18 *mm* from the centre and mesh size and absolute sag are 6.236 *mm* and 1.002 respectively and here also the red part which indicate the highest stress concentration located at the crack shown in Fig.7.

Fig. 7. Von Mises Stress Distribution of I-Beam

Not only point load consideration, we have also analyzed the same cracked I-beam model by applying rotational load to check the variation of stress in such cases whenever the same structure has to be subjected to an uniform torque or rotational loading. In this case shear stress also will be predominant rather than direct bending stress.

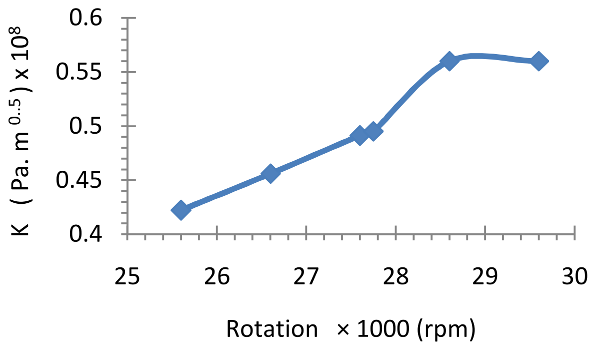

Fig. 8. Angular rotation Vs stress concentration factor (*K*) for I-Beam

Angular rotation Vs stress concentration factor (*K*) for I-Beam Result of the stress concentration factor and crack length has been shown in Table 4.

Table 4. Result Analysis on I-Beam Under Both Point Load and Rotational Force

Sl.	Load x 1000 (*rpm*)	Von Mises Stress (σ) N/m^2 x 10^8	Strain (x 10^{-3})	Principal Stress (N/m^2) x 10^8	Strain Energy (*J*)	(*K*) *Pa* $m^{1/2}$ x 10^{08}
1	25.6	2.13	35.9	2.33	3.63	0.422
2	26.6	2.30	38.4	2.52	4.23	0.456
3	27.6	2.48	40.9	2.68	4.91	0.491
4	27.75	2.50	41.3	2.74	5.02	0.495
5	28.6	2.66	43.6	2.91	5.66	0.56
6	29.6	2.85	46.3	3.12	6.49	0.56

Solid Circular Shaft

The model element is created in CATIA V5 with height 100 *mm* and radius 37.85 *mm* Fig. 9.

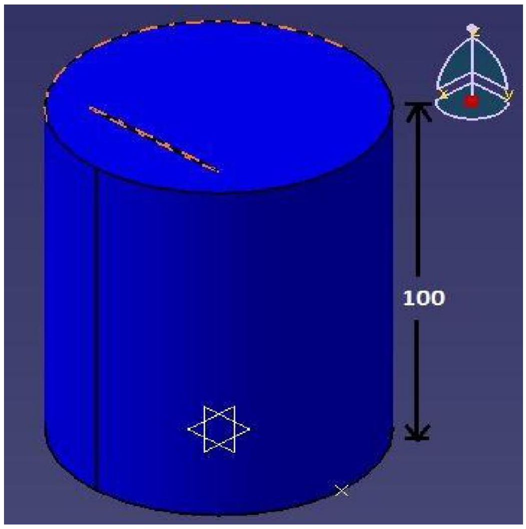

Fig. 9. Model of Solid Shaft

For rotational speed at 22000 *rpm* mesh size and absolute sag 6.236 *mm* and 1.002 *mm* the CATIA V5 analysis gives Fig.10.

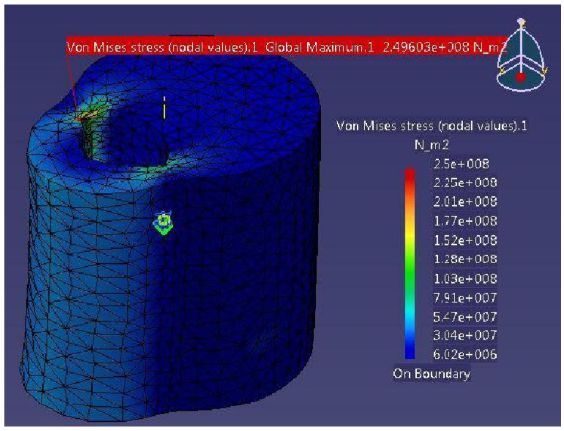

Fig. 10 . Von Mises Stress Distribution of Solid Shaft

The analysis from CATIA V5 has been shown in Table 5 for Solid Shaft. The red-colour marked row in this table indicates the critical stress concentration factor and critical crack length which is 40 mm.

Table 5. Result analysis on solid shaft

Sl. No.	Crack length (mm)	Von Mises Stress(σ) $N/m^2 \times 10^{08}$	(K) $Pa\ m^{1/2} \times 10^{08}$
1	20	0.92	0.163
2	30	1.00	0.271
3	40	2.50	0.626
4	50	2.12	0.594
5	60	2.89	2.11

The variation of stress concentration factor against the computational crack length reveals that there are abrupt rise in stress concentration factor, when the crack length reaches at its critical value as is evident from Fig.11.

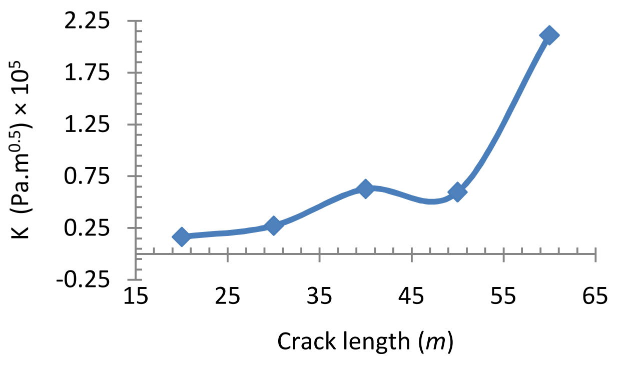

Fig. 11. Computational crack length vs. Stress Concentration Factor for solid shaft

Hollow Circular Shaft

The hollow shaft model created in CATIA V5 with 100 *mm* height and 39.15 *mm* inner diameter as shown in Fig.12. The other dimensions are same as earlier.

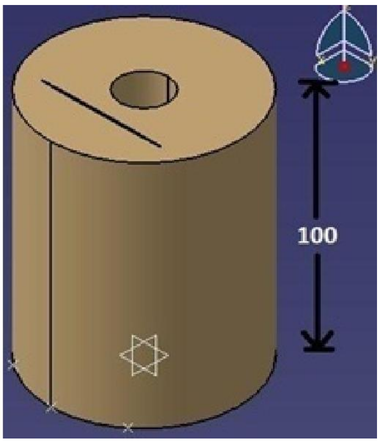

Fig. 12. Model of Hollow Shaft

The model is subjected to a rotation at an angular velocity of 2303.835 *rad/sec*. The crack is of elliptical in shape with the major and minor axis diameters of 62.36 *mm* and 1.002 *mm* respectively.

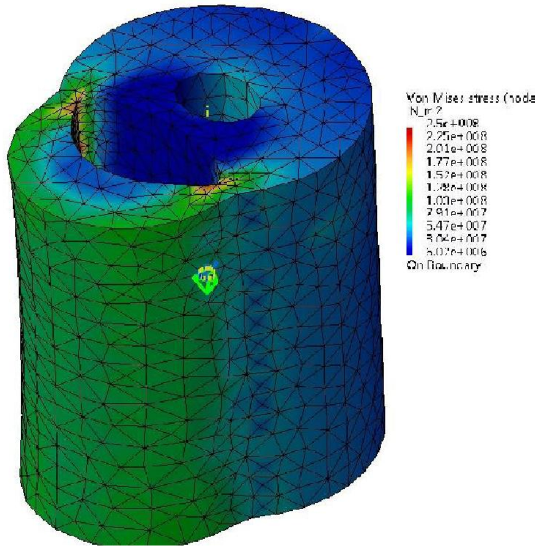

Fig. 13. Von mises stress distribution of hollow shaft

The analysis in the CATIA V5 gives the output for the crack propagation as shown in Fig.13 and Table 6.

Table 6. Result analysis on hollow shaft

Sl. No.	Crack Length (*mm*)	Stress (σ) $N/m^2 \times 10^8$	*(K)* $Pa\ m^{1/2} \times 10^{08}$
1	30	1.04	0.228
2	40	1.20	0.300
3	50	1.64	0.460
4	56	2.50	0.626
5	60	3.13	0.961

The variation of stress concentration factor against the computational crack length reveals that there are abrupt rise in stress concentration factor, when the crack length reaches at its critical value as is evident from Fig.14.

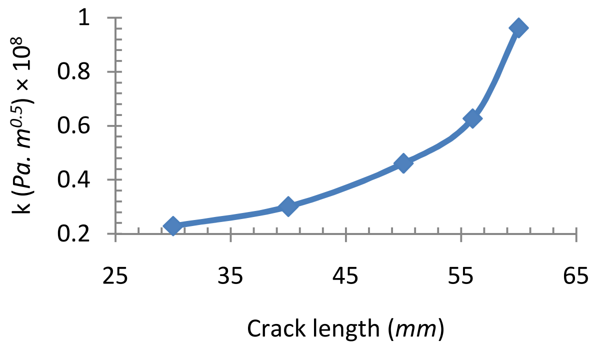

Fig. 14. Computational crack length vs. Stress Concentration Factor for hollow shaft

Now for point load 5000 *N* and varying rotational force both with crack type elliptical along the major diameter of 25 *mm* and minor diameter of 1 *mm* at a distance of 18 *mm* from the centre and mesh size and absolute sag 6.236 *mm* and 1.002 *mm*, the stress analysis of which in CATIA V5 is shown in Fig.15.

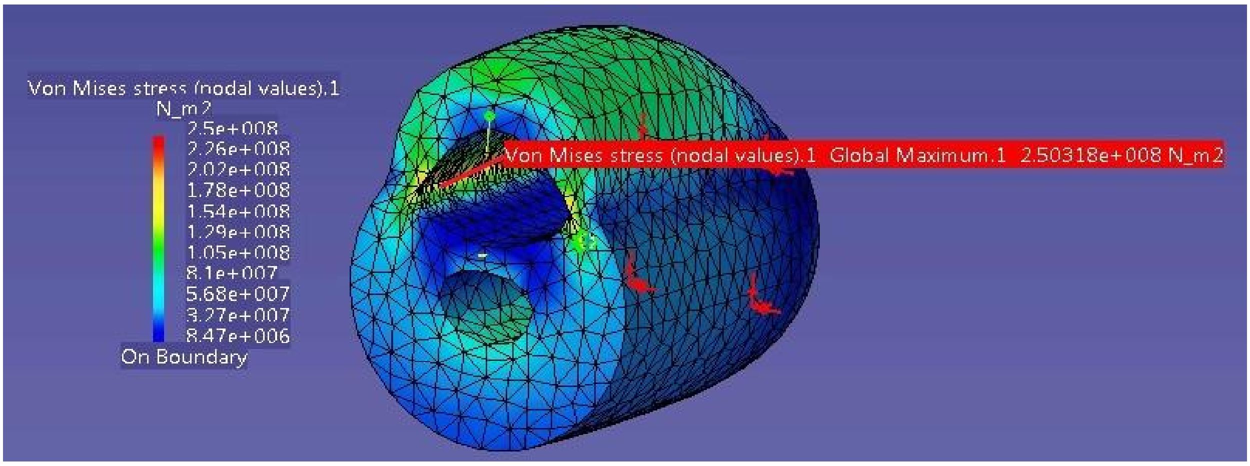

Fig. 15. Von mises stress distribution of hollow shaft

Moreover, the outputs for crack propagation are shown in Fig.16 and Table 7.

Table 7. Result analysis on hollow shaft under rotation

Sl. No.	Rotation x 1000 *rpm*	Von Mises Stress (σ) N/m^2 x 10^8	Strain (x 10^{-3})	Principal Stress (N/m^2) x 10^8	Strain Energy (*J*)	*(K)* $Pa\ m^{1/2}$ x 10^{08}
1	25.6	1.88	17.7	2.05	1.97	0.372
2	26.6	2.03	19.3	2.22	2.30	0.402
3	27.6	2.19	21.1	2.39	2.67	0.434
4	28.6	2.35	22.9	2.57	3.08	0.465
5	29.5	2.50	24.6	2.73	3.49	0.495
6	29.6	2.52	24.6	2.75	3.54	0.499

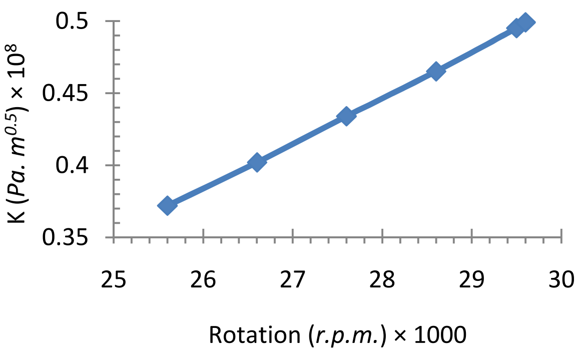

Fig. 16. Angular rotation Vs Stress concentration factor

Eccentric loading in hollow circular shaft

The model in Fig.12 is analysed in CATIA V5 with elliptical crack along the axis major axis diameter 25 *mm* and minor axis diameter 1 *mm* and at a distance of 18 *mm* from the centre having mesh size and absolute sag 6.236 *mm* and 1.002 *mm* respectively. The result from CATIA V5 is shown in Fig.16 and also in Table 8.

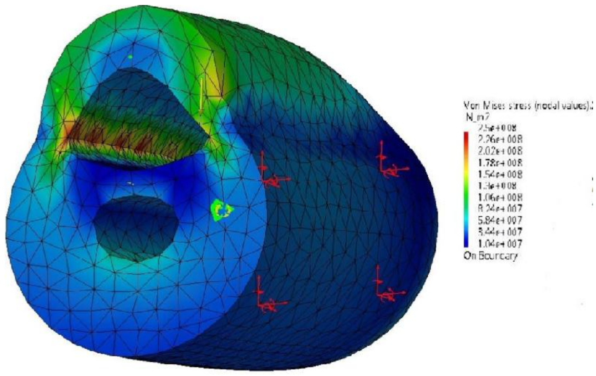

Fig. 17. Von mises stress distribution at crack propagation with eccentric loading 24 *mm*

The Von Mises stress developed in the structure is also studied under the combined simultaneous effect of point load of 5000 *N* under a uniform rotation of 29500 *rpm* when the eccentric load was applied at a radial offset distance of 24 *mm*.

Table 8. Analysis of eccentric loading on hollow shaft

Sl. No.	Rotation (*rpm*)	Eccentricity	Von Mises Stress N/m^2 x 10^8	*(K)* $Pa\ m^{1/2}$ x 10^{08}
1	29600	0	2.5	0.495
2	29800	12	2.5	0.495
3	29550	18	2.5	0.495
4	29500	24	2.5	0.495

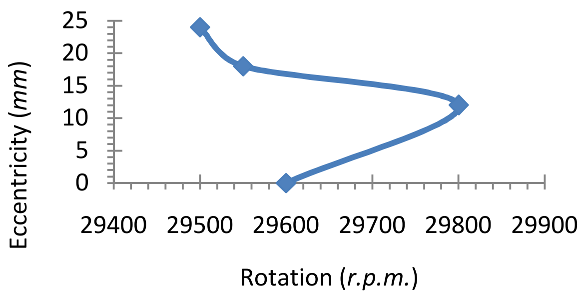

Fig. 18. Computational eccentricity VS angular rotation for hollow shaft

Discussions under Comparative Persepctive

First Case

It has been revealed from the comparative study (as shown in Table 9) between a rectangular beam and an I-beam under similar conditions that the I-beam is safer from rectangular beam in order to get rid of crack propagation.

Table 9. Comparison between rectangular beam and i-beam

Component	Stress (σ) N/m^2 x 10^8	*(K)* *Pa* $m^{1/2}$ x 10^{08}	Critical Crack length (*mm*)
Rectangular beam	2.50	0.99	98
I-Beam	2.50	0.99	100

Second Case

On the other hand, if we compare between a hollow and a solid circular shaft under the similar conditions, crack propagation will start earlier in case of solid circular shaft than in case of hollow circular shaft as is evident from Table 10.

Table 10. Comparison between solid and hollow shaft

Component	Stress (σ) N/m^2 x 10^8	*(K)* *Pa* $m^{1/2}$ x 10^{08}	Critical Crack length (*mm*)
Solid shaft	2.50	0.626	40
Hollow shaft	2.50	0.626	56

Table 11. Comparison between i-beam and hollow shaft

Component	Stress (σ) N/m^2 x 10^8	(*K*) Pa$m^{1/2}$ x 10^8	Critical load equivalent (*rad. / sec.*)
I-Beam	2.50	0.495	2904.50
Hollow Shaft	2.50	0.495	3087.67

Third Case

Finally, on comparison between I-beam and hollow shaft under similar stress field and stress concentration factor, it may be concluded that a hollow circular shaft is safer than an I-beam as it can withstand more amount of equivalent critical load as shown in Table 11.

Conclusion

As seen from the results the crack propagation varies from material to material and the crack propagation is nothing but the process of energy conversion where stress concentration factor or stress intensity factor is the unique parameter which represents the magnitude for stress field severity near a crack tip, it gives the measure of strength at the crack tip. From the result of the analysis on CATIA V5 software it has been seen that, I-beam is better than rectangular beam under point load. For rotational loading between hollow shaft and solid shaft, hollow shaft is better and between I-beam and hollow shaft also hollow shaft is better. Because of the crack length in hollow shaft is much higher than other structure taken so hollow shaft is better in engineering structure compare to I-beam.

REFERENCES

Curtin W. A., Deshpande V. S., Needleman A., Giessen Van der E., Wallin M., 2010. "Hybrid discrete dislocation models for fatigue crack growth".

Gürses Ercan, Miehe Christian, 2009. "A computational framework of three-dimensional configurational-force-driven brittle crack propagation". *Computer Methods in Applied Mechanics and Engineering*, *198*: *1413-1428.*

Hurley P.J., Evans W.J., 2007. "A new method for predicting fatigue crack propagation rates". *Materials Science and Engineering,* 466(1–2): 265-273.

Miserez A., Rossoll A., Mortensen A. 2004. "Investigation of crack-tip plasticity in high volume fraction particulate metal matrix composites". *Engineering Fracture Mechanics*, 71:2385-2406.

Sadananda K., Vasudevan A.K, 1997. "Short crack growth and internal stresses", *International Journal of Fatigue*, 19(93): 99-108.

Seweryn Andrzej, 1994. "Brittle fracture criterion for structures with sharp notches." *Engineering Fracture Mechanics,* 47(5):673-681.

Shimojo M., Chujo M., Higo Y., Nunomura S., 1993. "Effect of load ratio on the deformation behaviour of fatigue crack tips". *International Journal of Fatigue*, 15(6): 455-459.

Wang Zhiqiang, Nakamura Toshio, 2004. "Simulations of crack propagation in elastic–plastic graded materials". *Mechanics of Materials,* 36(7): 601-622.

****